AcuBot: A Robot for Radiological Interventions

Dan Stoianovici, Kevin Cleary, Alexandru Patriciu, Dumitru Mazilu, Alexandru Stanimir, Nicolae Craciunoiu, Vance Watson, and Louis Kavoussi

***Abstract*—We report the development of a robot for radiological percutaneous interventions using uniplanar fluoroscopy, biplanar fluoroscopy, or computed tomography (CT) for needle biopsy, radio frequency ablation, cryotherapy, and other needle procedures. AcuBot is a compact six-degree-of-freedom robot for manipulating a needle or other slender surgical instrument in the confined space of the imager without inducing image artifacts. Its distinctive characteristic is its decoupled motion capability correlated to the positioning, orientation, and instrument insertion steps of the percutaneous intervention. This approach allows each step of the intervention to be performed using a separate mechanism of the robot. One major advantage of this kinematic approach is patient safety. The first feasibility experiment performed with the robot, a cadaver study of perispinal blocks under biplanar fluoroscopy, is presented. The main expected application of this system is to CT-based procedures. AcuBot has received Food and Drug Administration clearance (IDE G010331/S1), and a clinical trial of using the robot for perispinal nerve and facet blocks is presently underway at Georgetown University, Washington, DC.**

***Index Terms*—Image-guided surgical intervention, robot-assisted surgery, surgical robot.**

I. Introduction

Surgical navigation systems have been shown to significantly enhance image-guided interventional procedures in a large variety of clinical applications [1]. Image-guided robots provide similar functionality and, in addition, include active manipulation of the instrument [2]. Two immediate advantages derived from this augmented capability are the increased precision of motion and reduction of radiation exposure. Image-guided surgical robotic systems, however, requires specialized robotic hardware, image registration, and guidance algorithms. Some specialized image-guided robots have been developed for ensuring patient safety while providing imager compatibility.

Minerva (Swiss Federal Institute of Technology, Lausanne and Zurich) is a computer tomography (CT)-guided, multifunction neurosurgical robot [3]. It operates inside a CT gantry with free longitudinal movement allowing cranial scans at any level. Under the physician's remote control, Minerva can manipulate two instruments and the tool for automatic penetration of the skin, skull, and meninges.

A remote center of motion (RCM)-based prototype robot designed for needle alignment inside a CT gantry was developed by researchers at Siemens [4]. The robot presents a small distal part made of radiolucent materials capable of actively orienting a procedure needle about a fixed location. A new CT fluoro-servoing algorithm was derived for targeting purposes. Needle insertion was then performed manually.

Another RCM-based robot designed for neurosurgical CT interventions was developed at the University of Tokyo, Tokyo, Japan [5]. The system has a relatively small size and mounts on the mobile table of the CT scanner.

A CT-integrated system for interventional procedures was recently reported by Yanof *et al.* [6]. Preliminary experiments have been conducted with a FS-O2N Kawasaki robot in animal experiments.

Our URobotics Laboratory [7] at The Johns Hopkins University, Baltimore, MD, has previously developed two modular robotic components: 1) the percutaneous access of the kidney (PAKY) radiolucent needle driver [8] and 2) the RCM [9], which is a small surgical module capable of needle orientation. These were successfully used in a clinical study [10] of CT-guided kidney, spine, liver, and lung procedures of biopsies and radio frequency (RF) ablation. This study also revealed the potential advantages and requirements of the new robot. The AcuBot robot described here uses revised PAKY and RCM modules while incorporating two newly designed components, an XYZ Cartesian stage and a passive S-Arm, mounted on a new "bridge" frame. The main characteristic of this robot compared to the other surgical systems is its optimized architecture for X-ray guided percutaneous interventions. Its structure is mechanically and electronically correlated to the steps of the clinical intervention.

(a) (b)

Fig. 1. (a) Front and (b) side views of the AcuBot mounted on a CT scanner.

II. The Manipulator

AcuBot consists of two components: a robotic manipulator and a control box. Fig. 1 shows two views of the robot mounted on a CT scanner. The base of the robot (2) provides a bridge-like structure over the table. This structure is attached to a table adapter (1) which is customized to fit the imager. The robot has a total of six degrees of freedom (DOF) configured for decoupled positioning, orientation, and instrument insertion, as presented in Fig. 2. This figure uses the same reference numbers as Fig. 1. The instrument (7) is loaded in PAKY (6), which is an active radiolucent needle driver (T translation). PAKY is held by the RCM [9] module (5). This module is capable of precisely orienting the instrument about two nearly perpendicular directions (R_X and R_Z) coincident at the RCM point, thus allowing a pivoting motion about that point.

Manuscript received June 10, 2002; revised January 15, 2003. This paper was recommended for publication by Associate Editor J. Troccaz and Editor R. Taylor upon evaluation of the reviewers' comments. This work was supported in part by the U.S. Army Medical Research Acquisition Activity (USAMRAA) under Grant DAMD17-99-1-9022 and in part by the National Cancer Institute (NCI) under Grant 1R21CA088232-01A1. Its contents are solely the responsibility of the authors and do not necessarily represent the official views of USAMRAA or NCI. This paper was presented in part at the Society for Urology and Engineering 17th Annual Meeting, Orlando, FL, May 25, 2002.

D. Stoianovici is with the Urology and Mechanical Engineering Departments, The Johns Hopkins University, Baltimore, MD 21224 USA (e-mail: dss@jhu.edu).

K. Cleary and V. Watson are with the Radiology Department, Georgetown University, Washington, DC 20057 USA.

A. Patriciu is with the Mechanical Engineering Department, The Johns Hopkins University, Baltimore, MD 21224 USA.

D. Mazilu is with URobotics, The Johns Hopkins University, Baltimore, MD 21224 USA.

A. Stanimir and N. Craciunoiu are with the Mechanical Engineering Department, University of Craiova, Craiova 1100, Romania.

L. Kavoussi is with the Urology Department, The Johns Hopkins University, Baltimore, MD 21224 USA.

Digital Object Identifier 10.1109/TRA.2003.817072

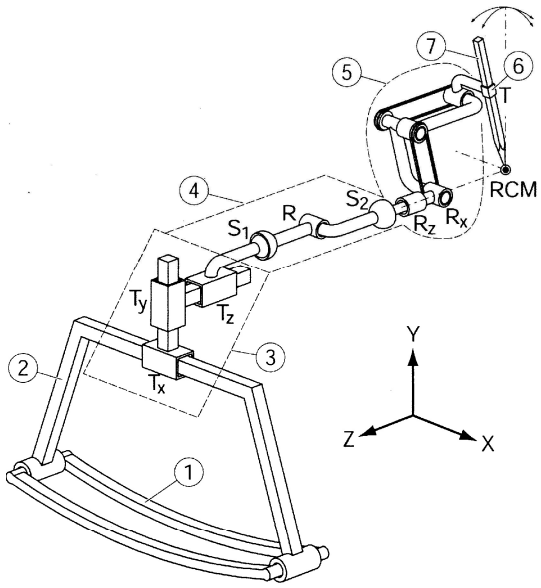

Fig. 2. Robot kinematics.

TABLE I
KINEMATIC SPECIFICATIONS

Axis	Resolution	Max. Velocity	Range of Motion
T	3 μm	50 mm/s	N/A
R_Z	0.003°	37 °/s	360°
R_X	0.006°	74 °/s	360°
T_X	2 μm	20 mm/s	200 mm
T_Y	2 μm	20 mm/s	50 mm
T_Z	2 μm	20 mm/s	50 mm

The remote R_X rotation axis through the RCM point is implemented by a two-belt parallelogram mechanism.

The RCM is supported by a passive positioning arm (4), called the S-Arm, with 7 DOF (S1 spherical, R revolute, S2 spherical). The arm can be positioned and rigidly locked from a single lever. The base of the arm (4) is mounted in a 3-DOF Cartesian stage (3), the XYZ module (T_X, T_Y, and T_Z translations).

While this stage uses commercially available ball-screws and linear slides, it is custom designed for the travel, speed, load, and compactness required for radiological interventions. For these reasons, this stage was built as part of the bridge structure (2). The key kinematic specifications of the AcuBot are given in Table I.

The user interface consists of a 15" resistive touch screen (8), a two-axis joystick, a switch panel (10), and an emergency stop button (11). These components are mounted on the front side of the bridge. A speaker (9) and the cable connector (12) are located on its back side.

III. CONTROL UNIT

The robot is connected to a control unit with a single custom cable incorporating multiple shields for the different groups of signals. The unit is entirely housed within a single industrial PC chassis. Several monitoring circuits, disabling, and emergency switches are used for safety (Fig. 3).

The PC uses a Dual Pentium III, 800-MHz motherboard with network and video adapters and standard HD, FD, and CD components. On-board motion control is implemented by an ISA-DSP card, PCX-DSP8 by Motion Engineering, Inc. The motion control card commands six linear amplifiers, 4-Q-DC by Maxon Precision

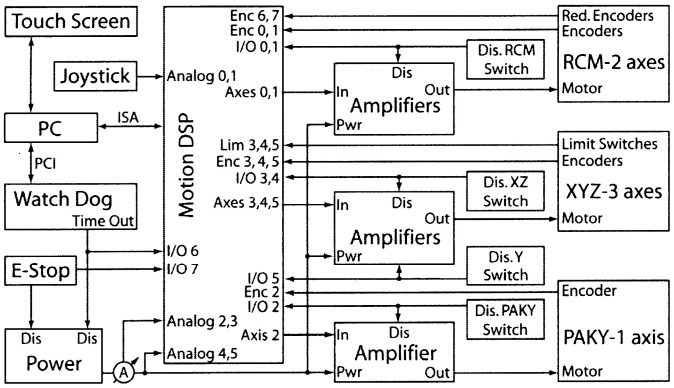

Fig. 3. Control block diagram.

Motor, Inc., powered by two 24 V, 100 W dc supplies. The voltage and load of the power supplies are monitored using current sensors (LTS 6-NP by LEM USA). The controller axes are clustered in four groups that can be individually enabled. Enable amplifier signals and relays (CIO-ERB24 by Computer Boards, Inc.) on the motor lines are controlled by input/output (I/O) ports on the motion card for this purpose. Disabling switches are also available on each group of axes to hardware override their activation, which is normally set by software.

The RCM module incorporates redundant encoders which are monitored by the main processor through the motion controller. The encoder indexes are used for zeroing the RCM mechanism. The axes of the Cartesian stage include limit switches for safety and a zero reference. The PAKY module uses a laser beam pointing at the instrument as a zero reference.

A watchdog protocol monitors the activity of the CPU control program, the state of the power voltages and currents, the state of the axes disable switches, and the emergency stop button. If no fault is detected, the control program updates the register of a watchdog countdown timer every 100 ms. If not updated, the counter sets its I/O pin low, which triggers the motion controller to shut down power.

IV. PERCUTANEOUS ACCESS SEQUENCE

The table adapter is initially mounted on the table of the imager and the robot is attached to it. The patient can enter from either side of the table by opening the bridge. A sterile PAKY driver and the procedure instrument/needle are mounted so that the tip of the needle is at the RCM point, which is highlighted by the laser beam. The passive arm is then manipulated to be close to the intervention site and firmly locked.

The physician can access the system from either the touch-screen monitor next to the patient or from a second input device directly attached to the computer located in the imager's control room. Registration and imaging are performed next, according to the method of choice. For X-xay fluoroscopy, we either use manual joystick control [8], or our fluoro-servoing algorithm [11] that we previously implemented [12] on the simpler PAKY-RCM system. For CT, we use the laser registration method [13], which is based on aligning the needle with the laser marks of the CT scanner.

Using either modality, the tip of the needle is then driven to the desired skin entry point using the XYZ stage. This is performed in two steps, starting with a horizontal plane motion (T_X, T_Z) above the patient, followed by a vertical move (T_Y). In the third step, the RCM module is used to orient the needle about this point (R_Z, R_X about RCM). Finally, the needle is inserted (T) using the PAKY driver, after proper targeting is confirmed by the physician. Thus, percutaneous access is achieved in four independent steps.

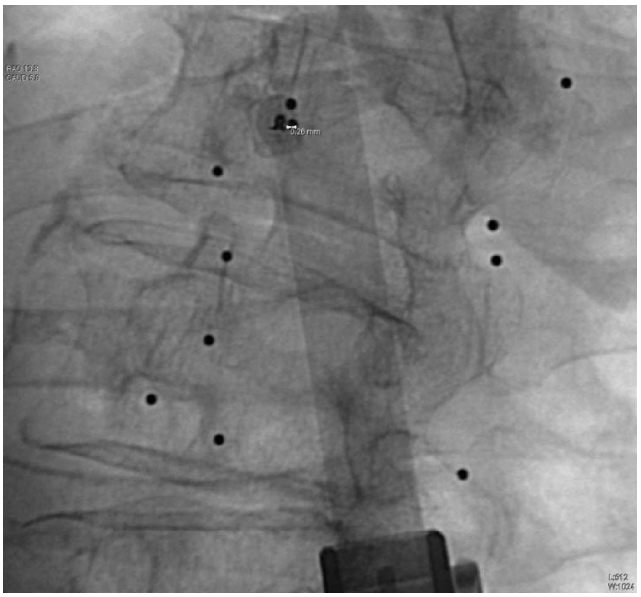

Fig. 4. A/P fluoroscopy for facet block at left L1-2.

V. Mechanic and Electronic Safety Features

The four-step sequence of the intervention is directly correlated with the manipulator's mechanical decoupling of motion and the electronic grouping of axes enabling their independent activation. With this, four separate mechanisms with independent control are used to perform horizontal and vertical positioning, orientation, and instrument insertion. This safety feature allows the control to sequentially enable groups of axes so that only the active mechanism is enabled in each sequence. For example, this ensures that the needle is not inadvertently inserted during the orientation step, since in that step, the XZ, Y, and PAKY (needle drive) axes are disabled.

Mechanically, all axes of the robot are highly geared, thus presenting minimal backdrivability. Vertical motion is gravity balanced, ensuring that the robot will stop should an emergency, computer crash, or even a power loss occur. Other safety features are: 1) the robot has minimal mechanical power; 2) its high gearing insures low maximum speeds; and 3) the workspace of the manipulator is small yet sufficient for the intervention.

VI. Cadaver Study

To evaluate the feasibility of using the AcuBot for radiological interventions, a cadaver study was completed in the interventional suite at Georgetown University [14]. The procedure selected was perispinal nerve and facet blocks, which require the physician to precisely place a 22-gauge needle into the spinal region under biplanar fluoroscopy. This procedure was selected as a good starting experiment for the robot, since it can be typically completed without difficulty by an experienced radiologist. The results of the cadaver study have also been used as preliminary clinical data for regulatory purposes.

In this study, a 98-year-old embalmed female cadaver was placed on the interventional table in a supine position. To serve as targets, 12 metal balls of 1-mm diameter were placed in the lumbar spine from vertebra L1 to L4, as presented in Fig. 4.

The experiment was entirely performed under joystick control using needle superimposition over the target in anterior/posterior (A/P) fluoroscopy, followed by needle insertion in lateral fluoroscopy [8]. As each needle was placed, the A/P and lateral fluoroscopy images were saved for follow-up analysis. Placement error was measured by the distance between the needle point and the target in each experiment, and the results are presented in Table II. The average placement error was 1.44 mm with a standard deviation of 0.66 mm, which was considered accurate by the radiologist. The errors were attributed to cumulative manual targeting errors and small needle/tissue deflection.

TABLE II
Targeting Error in Cadaver Study

Target #		Level	A/P Error [mm]	Lateral Error [mm]	Total Error [mm]
NERVE	1	Right 4	1.10	1.70	2.02
	2	Right 3	0.00	1.71	1.71
	3	Right 2	0.00	0.80	0.80
	4	Left 2	1.75	1.34	2.20
	5	Left 3	2.50	0.19	2.51
	6	Left 4	1.40	0.74	1.58
FACET	1	L1-2 Left	0.26	0.29	0.39
	2	L2-3 Left	0.96	1.53	1.81
	3	L3-4 Left	1.49	0.19	1.50
	4	L3-4 Right	0.70	0.13	0.71
	5	L2-3 Right	0.80	0.00	0.80
	6	L1-2 Right	0.00	1.19	1.19
Average			0.91	0.82	1.44
Standard Deviation			0.79	0.65	0.66

In this joystick-guided procedure, the benefits of using the robot were: 1) the needle can be oriented and inserted with ease and precision; 2) the trajectory of the needle is enforced by the robot rather than having the physician attempting to manually maintain it; 3) the physician can view the location and trajectory of the needle in real time since his/her hand is not in the path of the X-ray beam; and 4) the needle does not perceivably deflect or sag as it might in the manual procedure.

VII. Conclusion

AcuBot is optimized for percutaneous access, achieving compactness without loss of maneuverability within the imager. Its bridge mounting on the imager table gives a sturdy and ergonomic support that preserves the relative positioning of the robot and patient, which is especially valuable with scanner-type imagers. Its structure provides flexibility in performing interventions at any location of the body and with different imaging modalities. AcuBot's safety features were designed based on observation of common interventions performed by experienced radiologists. The cadaver study shows the feasibility of using this system in a basic joystick experiment. Clinical trials are currently underway at Georgetown University. A respiratory motion-tracking algorithm and a new instrument driver for minimizing soft tissue and needle deflection are some of our current research topics.

References

[1] H. Reinhardt, M. Trippel, B. Westermann, and O. Gratzl, "Computer aided surgery with special focus on neuronavigation," *Comput. Med. Imag. Graph.*, vol. 23, pp. 237–44, 1999.

[2] D. Stoianovici, "Robotic surgery," *World J. Urol.*, vol. 18, pp. 289–95, 2000.

[3] J. L. Hefti, M. Epitaux, D. Glauser, and H. Fankhauser, "Robotic three-dimensional positioning of a stimulation electrode in the brain," *Comput.-Aided Surg.*, vol. 3, pp. 1–10, 1998.

[4] M. H. Loser and N. N., "A new robotic system for visually controlled percutaneous interventions under CT fluoroscopy," in *Proc. LNCS*, vol. 1935, 2000, pp. 887–896.

[5] K. Masamune, L. H. Ji, M. Suzuki, T. Dohi, H. Iseki, and K. Takakura, "A newly developed stereotactic robot with detachable driver for neurosurgery," in *Proc. MICCAI*, vol. 1496, 1998, pp. 215–222.

[6] J. Yanof, J. Haaga, P. Klahr, C. Bauer, D. Nakamoto, A. Chaturvedi, and R. Bruce, "CT-integrated robot for interventional procedures: Preliminary experiment and computer-human interfaces," *Comput.-Aided Surg.*, vol. 6, pp. 352–9, 2001.

[7] D. Stoianovici, "URobotics—Urology robotics at Johns Hopkins," *Comput.-Aided Surg.*, vol. 6, pp. 360–369, 2001.

[8] D. Stoianovici, J. A. Cadeddu, R. D. Demaree, S. A. Basile, R. H. Taylor, L. L. Whitcomb, W. N. Sharpe, and L. R. Kavoussi, "An efficient needle injection technique and radiological guidance method for percutaneous procedures," in *Proc. LNCS*, vol. 1205, 1997, pp. 295–298.

[9] D. Stoianovici, L. L. Whitcomb, J. H. Anderson, R. H. Taylor, and L. R. Kavoussi, "A modular surgical robotic system for image guided percutaneous procedures," in *Proc. LNCS*, vol. 1496, 1998, pp. 404–410.

[10] S. B. Solomon, A. Patriciu, M. E. Bohlman, L. R. Kavoussi, and D. Stoianovici, "Robotically driven interventions: A method of using CT fluoroscopy without radiation exposure to the physician," *Radiology*, vol. 225, pp. 277–282, 2002.

[11] A. Patriciu, D. Stoianovici, L. L. Whitcomb, T. Jarrett, D. Mazilu, A. Stanimir, I. Iordachita, J. Anderson, R. Taylor, and L. R. Kavoussi, "Motion-based robotic instrument targeting under C-Arm fluoroscopy," in *Proc. LNCS*, vol. 1935, 2000, pp. 988–998.

[12] L. M. Su, D. Stoianovici, T. W. Jarrett, A. Patriciu, W. W. Roberts, J. A. Cadeddu, S. Ramakumar, S. B. Solomon, and L. R. Kavoussi, "Robotic percutaneous access to the kidney: Comparison with standard manual access," *J. Endourology*, vol. 16, pp. 471–475, 2002.

[13] A. Patriciu, S. Solomon, L. R. Kavoussi, and D. Stoianovici, "Robotic kidney and spine percutaneous procedures using a new laser-based CT registration method," in *Proc. LNCS*, vol. 2208, 2001, pp. 249–258.

[14] K. Cleary, D. Stoianovici, A. Patriciu, D. Mazilu, D. Lindisch, and V. Watson, "Robotically assisted nerve and facet blocks: A cadaveric study," *Acad. Radiology*, vol. 9, pp. 821–825, 2002.